

Numerical Analysis of the Effect of Combustor Length on Cylindrical Rotating Detonation Engine with Diverging Channel

Takumi Sada¹, Akiko Matsuo², Eiji Shima²,
Noboru Itouyama³, Akira Kawasaki⁴, Ken Matsuoka³, Jiro Kasahara³

¹Graduate School of Science and Technology, Keio University
Yokohama, Kanagawa, Japan

²Department of Mechanical Engineering, Keio University
Yokohama, Kanagawa, Japan

³Department of Aerospace Engineering, Nagoya University
Nagoya, Aichi, Japan

⁴Department of Mechanical Engineering, Shizuoka University
Hamamatsu, Shizuoka, Japan

1 Introduction

Rotating detonation engine (RDE) has been getting attention as a novel heat engine. Detonation in this engine can provide high theoretical thermal efficiency [1,2] and is expected to reduce the size of the combustor due to the compression effect by the shock wave and the rapid completion of combustion. In the typical RDE, detonation propagates through the unburned gas from the bottom of the annular combustor. The expansion after the combustion accelerates the burned gas in the axial direction, and it is exhausted from the combustor outlet. However, RDE has problems to practical use. One of the problems is the high heat load on the combustor walls [3,4]. To solve this problem, the combustor without inner wall is proposed and it is confirmed this engine can provide similar propulsive performance with an annular RDE in the experiments [5]. This type of engine is called as cylindrical or hollow RDE. Numerical analysis has also confirmed that detonation can propagate in such an RDE [6,7].

In addition, to obtain greater propulsive performance with simple geometry, which is one of the advantages of RDE, the cylindrical RDE with diverging channel is proposed by Nakata et al. [8]. In the RDE, the distance to complete combustion is short, so the flow can be choked only by the heat generated by detonation. Taking advantage of this, the combustor with diverging channel is expected to obtain supersonic exhaust and improvement of propulsive performance. In this previous research, the Mach number estimated with measured pressure and exhaust plume was 1.5-1.7, so the supersonic exhaust

was experimentally confirmed. This is the new type of combustor geometry to achieve high propulsive performance with simple geometry. However, there is not enough knowledge about the internal flow and detonation propagation in RDE.

This study investigates the influence of diverging channel on the internal flow and propulsive performance in cylindrical RDE. In this report, the cylindrical RDE with constant diverging angle 5° is numerically analyzed with hydrogen-air premixed gas injection. Three types of the combustor length 20 mm, 50 mm, and 70 mm are examined. From the results, we investigate the effects of combustor length in diverging channel and compare the results with straight channels.

2 Numerical Setup

The governing equations were three-dimensional compressible Euler equation with mass conservation of nine species (H_2 , O_2 , H , O , OH , H_2O , HO_2 , H_2O_2 , N_2). Also, to enclose the system, the equation of state was used assuming thermally perfect gas condition. The thermodynamic properties were calculated with NASA polynomials [9]. The convective term is discretized by AUSMDV [10], which third ordered by MUSCL method. The fluid time integration is performed with three-stages third order TVD Runge-Kutta method [11], and courant number was 0.3. The time integration for the source term was performed with the Point Implicit method. The time step for chemical reaction was divided into five steps to make the time step small enough to allow stable calculation. The chemical reaction model proposed by Hong et al. [12], which considers 20 elementary reactions, was used to consider the reaction of H_2 - O_2 .

Figure 1 shows the computational domain. The size of the combustor was the same as that of the combustor used in the experiment by Nakata et al. [8], with a bottom diameter of $d_0 = 20$ mm and a diverging angle of 5° . The diameter of the injectors was 1.2 mm, and 24 injector pairs were arranged in the circumferential direction. While fuel and oxidizer are usually supplied separately to prevent backfire, premixed gas was injected in this analysis excluding the mixing effect. To simulate the flow field formed by the pair of injectors, two rows of injectors were arranged so that the premixed gas collided at an angle of 90° , as shown in Fig. 1(c). The center of the injectors located at $r = 8.5$ mm and 6.5 mm. In this report, in order to numerically analyze a cylindrical combustor without inner wall, the annular and cartesian grids were overlapped, and the values were interpolated in $r - \theta$ plane. The number of grid points of annular region in the θ and r directions was 1001 and 97 respectively, and that of cartesian grid was 311 and 311. In this analysis, the length of the combustor was varied from 20 mm, 50 mm, and 70 mm, and the number of grid points in the length z direction is 398, 786, and 888, respectively. The total number of grid point is 172 Mpts. in 70 mm case. The grid width ranged from 25 to 67 μ m at the bottom.

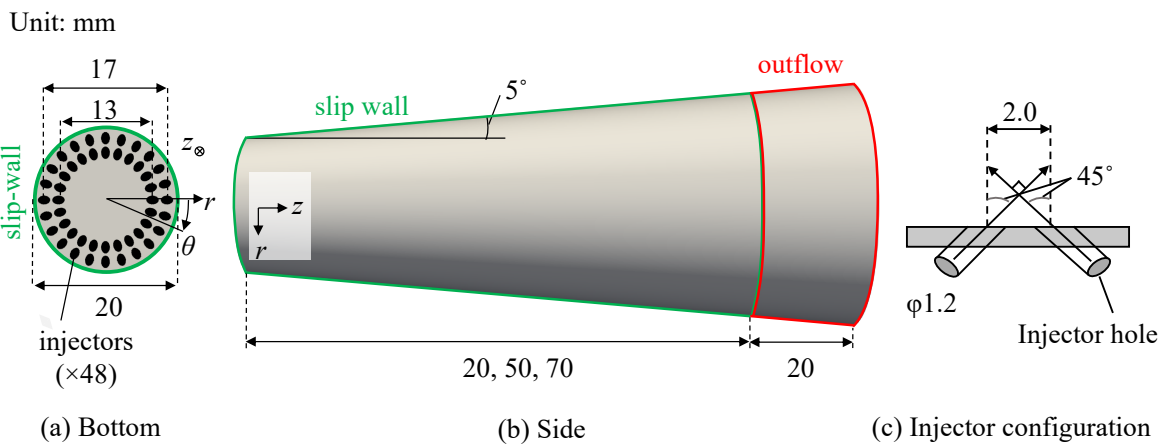


Figure 1: Computational domain and boundary conditions. (a) bottom of the combustor, (b) side of the combustor, and (c) injector configuration.

The boundary conditions are following. On the injector surface, the total pressure and temperature were set to 1.000 MPa and 298.15 K, respectively, and premixed gas composition of $2\text{H}_2\text{-O}_2\text{-3.76N}_2$ was applied. A slip wall condition was applied on the combustor walls. The external pressure was set to a constant pressure of 10 kPa for a subsonic outflow. The choked inflow conditions are 0.528 MPa and 248.4 K. In this condition, the C-J velocity and the induction length were calculated as 2012 m/s and 201.9 μm , respectively.

3 Results and Discussion

Figure 2 shows instantaneous temperature fields and isosurfaces of pressure and H_2 mole fraction for each length with the results of 70 mm combustor without diverging angle. In Fig. 2(a), all cases show the propagation of a detonation with large temperature increase. The characteristics of the temperature field observed on the outer wall were as follows. The low-temperature unburned mixture was observed near the bottom and behind the detonation. A detonation is propagating through that unburned mixture, with a oblique shock extending from the filling height of the unburned mixture. In the 20 mm combustor, the oblique shock is not clear due to the short combustor, but the above features are similar for all cases. Comparing these features with those of the straight channel in Fig. 2(a), the temperature behind the detonation is lower in diverging channel, and there is a difference in the appearance of unburned gas pockets seen on the outer wall. The unburned gas pockets are observed over a wide area behind the wave with the diverging angle, whereas such gas pockets are rarely observed in the straight channel. To observe the three-dimensional distribution of detonation and unburned gas, Fig. 2(b) shows the isosurfaces of pressure and mole fraction of H_2 . The pressure was shown every 0.25 MPa from 1.0 MPa to 3.0 MPa, and the mole fraction of H_2 showed the isosurface of 0.29. The pressure surfaces indicate

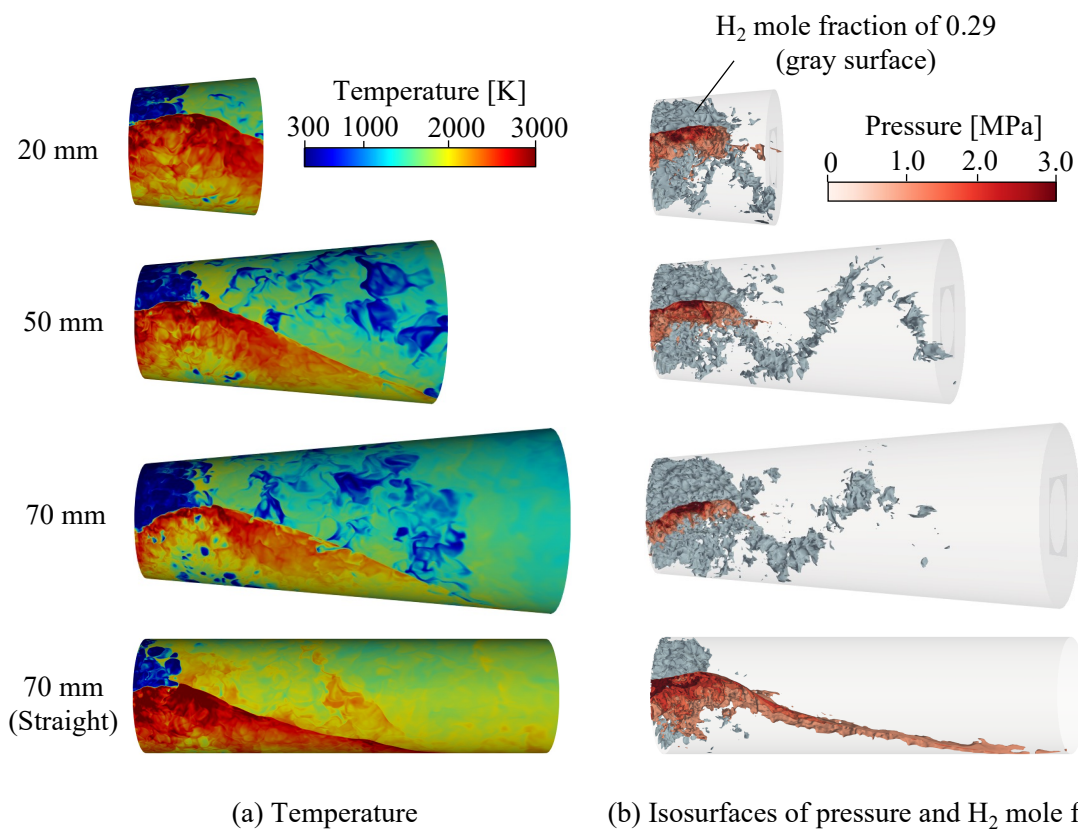


Figure 2: Instantaneous (a) temperature fields and (b) isosurfaces of pressure every 0.25 MPa from 1.0 MPa to 3.0 MPa and mole fraction of H_2 0.29.

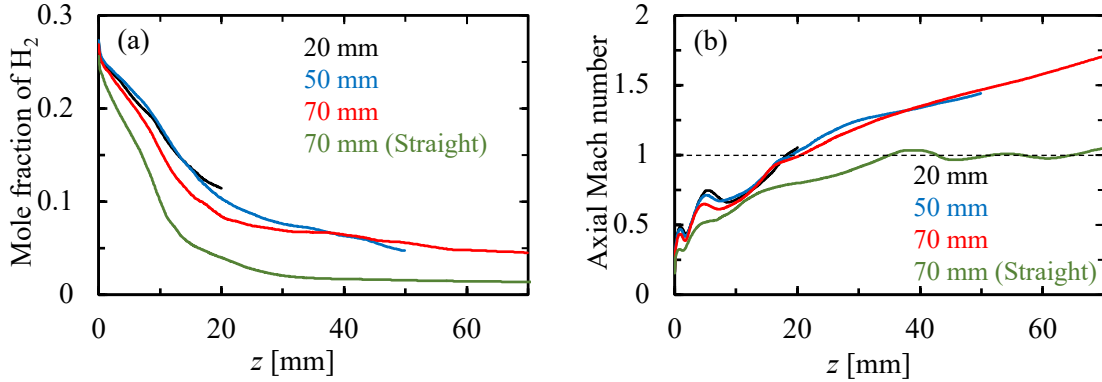


Figure 3: Spatiotemporal average profiles of (a) mole fraction of H_2 and (b) axial Mach number.

the regions of high pressure, especially propagating wave in the channel. In the case with diverging angle, there is no significant difference in the height of the pressure surfaces. On the other hand, the surface in straight channel shows larger high-pressure region with clear oblique shock. The gray surface with a mole fraction of H_2 0.29 shows the unburned mixture flowed from the bottom. As seen in Fig. 2(b), the unburned pockets are distributed in a spiral shape in the diverging channel. This is not observed in straight channel as with temperature field in Fig. 2(a).

Figure 3 shows the spatiotemporal average profiles in axial direction during one lap of wave propagation. Figure 3(a) shows the axial profile of mole fraction of H_2 . In Fig. 3(a), the H_2 consumption toward the combustor outlet is different for the diverging channel compared to the straight one. In the straight channel, a large consumption is observed to $z = 15$ mm. However, the diverging channel shows the gradual fuel consumption toward the combustor outlet. This also indicates that there the diverging channel shows the larger amount of unburned gas pocket behind the wave. Figure 3(b) shows the axial Mach number profile. In the diverging channel, the axial Mach number exceeds 1 around $z = 18$ mm, continuing to accelerate. Table 1 shows the Mach number at the exit and propulsive performances. As in Table 1, the average Mach number at the exit is 1.05 in 20 mm, 1.44 in 50 mm, and 1.71 in 70 mm combustor. For the 70 mm case, where the bottom diameter, diverging angle, and combustor length are equal to those in the previous experiment [8], the trend is consistent with the experimentally estimated range of 1.5 – 1.7 for the exit Mach number. Thus, the supersonic exhaust in a simple combustor experimentally obtained in previous studies was also confirmed in the numerical analysis.

To compare the propulsive performance, Fig. 4 shows the thrust F to combustor length and the components are shown in Table 1. These values were averaged during two laps propagation. The control surface method [13] was used to calculate the thrust, with the combustor bottom and side wall as control surface. F_m is the momentum thrust, F_p is the pressure thrust. Figure 4 shows that the thrust is increase with combustor length in diverging channel. This is due to the continuous acceleration in the diverging channel. In addition, the component of thrust in Table 1 shows the increase in $F_{p,wall}$ in particular. This $F_{p,wall}$ is evaluated only by area change and wall pressure. From the above, it is thought that the approximate trend of thrust for diverging channel can be obtained by capturing the trend of the change in pressure. Therefore, we investigated the prediction of wall pressure and Mach number using a simple model and its accuracy. Here, isentropic flow near the combustor outlet is assumed and a quasi-one-dimensional steady flow is analyzed. The equations are the conservation of mass, momentum, isentropic formula, and equation of state. With these equations, the changes in Mach number and pressure to the area increase can be obtained as in Eq. (1) and Eq. (2). M is Mach number, γ is specific heat ratio, A is area, and p is pressure.

$$\frac{dM}{M} = \frac{2 + (\gamma - 1)M^2}{2(M^2 - 1)} \frac{dA}{A} \quad (1)$$

Table 1: Mach number at exit and thrust.

Case	Mach at exit	Thrust F [N]	F_m [N]	$F_{p,\text{bottom}}$ [N]	$F_{p,\text{wall}}$ [N]
20 mm	1.05	152±3	26.7±0.3	98.1±2.8	27.4±1.1
50 mm	1.44	176±7	26.7±0.3	99.3±4.4	49.9±2.7
70 mm	1.71	184±3	26.8±0.3	98.7±5.5	58.6±4.3
70 mm (Straight)	1.05	167±8	25.1±0.6	142±8	-

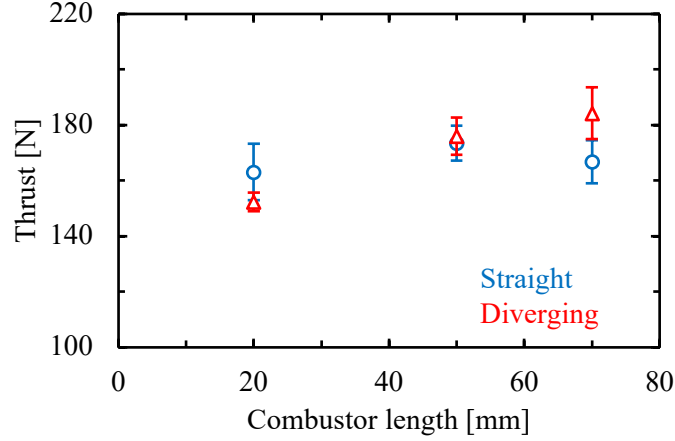


Figure 4 Thrust to combustor length.

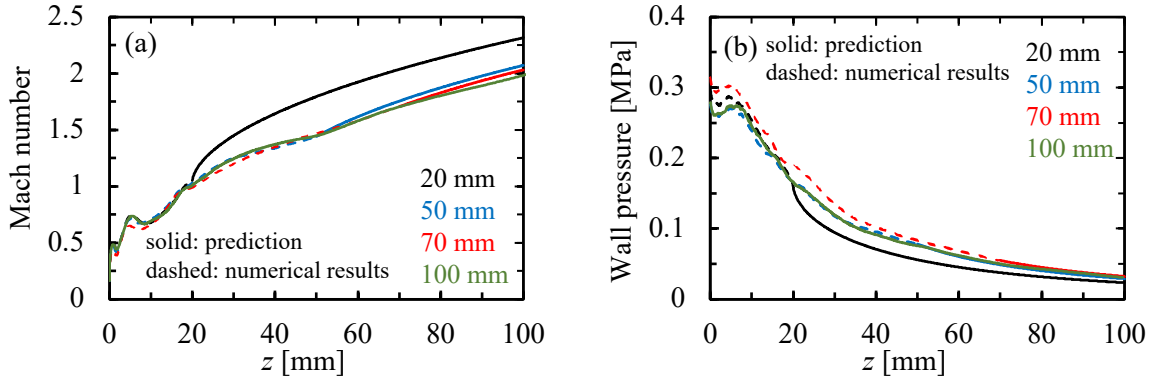


Figure 5 Prediction of (a) Mach number and (b) wall pressure.

$$\frac{dp}{p} = -\frac{\gamma M^2}{M^2 - 1} \frac{dA}{A} \quad (2)$$

Using these equations with the values at combustor exit in each length, the Mach number and wall pressure are predicted. The analysis was performed to $z = 100$ mm with a step width $\Delta z = 0.1$ mm and constant specific heat ratio $\gamma = 1.25$. Figure 5 shows the results of this prediction with 100 mm results in numerical simulation. The dashed lines show the results of numerical analysis, and the solid lines show that of the prediction. In Fig. 5, the results with the 20 mm combustor show an underestimation of pressure and an overestimation of Mach number compared to other combustors. The difference is not significant in 50 mm and 70 mm combustor. This is due to the fact that the heat release in the 20 mm combustor is not enough progressed as seen in H_2 profile in Fig. 3(a). From these results, it is considered possible to predict the flow and thrust trend by using values well behind the combustion zone. This indicates the possibility to obtain a flow structure with one numerical result in this geometry.

4 Summary

In this report, a series of inviscid numerical analysis on cylindrical rotating detonation engine with diverging channel is conducted. The average axial Mach number reached 1 at around $z = 18$ mm for all combustor lengths. The Mach number at the exit was 1.71 for the 70 mm combustor, which was consistent with a previous study with the same geometry. The propulsive performance with diverging channel depends on the length, and the trend of flow and thrust can be predicted by simple analysis with the results of well behind the combustion zone.

Acknowledgments

This study was financially supported by JSPS KAKENHI Grants No. JP19H05464 and by the Institute of Space and Astronautical Science of the Japan Aerospace Exploration Agency. Part of the numerical results in this research were obtained using supercomputing resources at Cyberscience Center, Tohoku University.

References

- [1] Zeldovich YB. (2006). To the Question of Energy Use of Detonation Combustion. *Journal of Propulsion and Power*. 22: 3.
- [2] Wolański P. (2013). Detonative Propulsion. *Proc. Combust. Inst.* 34: 1.
- [3] Bykovskii FA. Vedernikov EF. (2009). Heat Fluxes to Combustor Walls during Continuous Spin Detonation of Fuel-Air Mixtures. *Combustion, Explosion, and Shock Waves*. 45: 1.
- [4] Braun J. Sousa J. Paniagua G. (2018). Numerical Assessment of the Convective Heat Transfer in Rotating Detonation Combustors Using a Reduced-Order Model. *Applied Sciences* 8: 6.
- [5] Yokoo R. Goto K. Kim J. Kawasaki A. Matsuoka K. Kasahara J. Matsuo A. Funaki I. (2020). Propulsion Performance of Cylindrical Rotating Detonation Engine. *AIAA Journal*. 58: 12.
- [6] Tang XM. Wang JP. Shao YT. (2015). Three-Dimensional Numerical Investigations of the Rotating Detonation Engine with a Hollow Combustor. *Combustion and Flame*. 62: 4.
- [7] Yao S. Tang X. Luan M. Wang J. (2017). Numerical Study of Hollow Rotating Detonation Engine with Different Fuel Injection Area Ratios. *Proc. Combust. Inst.* 36: 2.
- [8] Nakata K. Ota K. Ito S. Ishihara K. Goto K. Itouyama N. Braun J. Meyer T. Paniagua G. Lafayette W. (2022). Supersonic Exhaust from a Rotating Detonation Engine with Throatless Diverging Channel. *AIAA Journal*.
- [9] McBride BJ. Gordon S. Reno MA. (1993). Coefficients for Calculating Thermodynamic and Transport Properties of Individual Species. NASA Technical Memorandum. 4513.
- [10] Wada Y. Liou M. (1997). An Accurate and Robust Flux Splitting Scheme for Shock and Contact Discontinuities. *SIAM Journal on Scientific Computing*. 18: 3.
- [11] Gottlieb S. Shu CW. (1998). Total Variation Diminishing Runge-Kutta Schemes. *Mathematics of Computation*. 67: 221.
- [12] Hong Z. Davidson DF. Hanson RK. (2011). An Improved H₂/O₂ Mechanism Based on Recent Shock Tube/Laser Absorption Measurements. *Combustion and Flame*. 158: 4.
- [13] Shepherd JE. Kasahara J. (2017). Analytical Models for the Thrust of a Rotating Detonation Engine. GALCIT Report. FM2017.001.